Supplementary Data

Organically tuned white-light emission from two zero-dimensional Cd-based hybrids

Rawia Msalmi,[a] Slim Elleuch,[b] Besma Hamdi,[c] Wesam. Abd El-Fattah, [d,e] Naoufel Ben Hamadi [d,f] and Houcine Naïli *[a]

Table S1. Crystallographic data and structural refinement parameters of CdODA

Crystallographic data	
Chemical formula	$(C_{12}H_{13}N_2O)_2CdBr_4$
Formula weight M_r	836.51
Crystal system Space group	Monoclinic $P2_1/c$
a (Å) *b* (Å) *c* (Å)	14.783 (4) 12.746 (2) 16.051 (3)
β (°)	107.908 (6)
V (Å^3)	2877.9 (11)
Z *F*(000)	4 1600
μ (Mo *K*α) (mm^{-1}) Morphology	6.34 Needle
Crystal color	Brown
Intensities measurements	
Temperature (K) Mo *K*α (Å) θ Range for data collection (°) h, k, l ranges Reflections collected	296 0.71073 2.9–19.6 −17≤ h ≤17 −14≤ k ≤15 −19≤ l ≤19 21375
Structural Determination	
Absorption correction Refinement method T_{max} T_{min} independent reflections R_{int} Observed reflections [$I > 2\sigma(I)$] R1 wR_2 Goof (S)	Multi-scan Full-matrix least Squares on F^2 0.467 0.245 5393 0.069 3174 0.039 0.078 0.97

Table S2. Geometric data of intermolecular hydrogen bonds of $[H(ODA)]_2\ CdBr_4$

D—H···A	D—H(Å)	H···A(Å)	D···A(Å)	D—H···A(°)
N1—H1A···Br1	0.86	2.73 (4)	3.577 (6)	169 (3)
N2—H2A···Br3^{i}	0.89	2.7000	3.334 (4)	129.00
N2—H2B···N3^{ii}	0.89	2.3400	2.847 (7)	116.00
N2—H2B···Br1^{iii}	0.89	2.7200	3.402 (5)	135.00
N2—H2C···Br4^{iv}	0.89	2.6700	3.558 (4)	175.00
N3—H3B···Br2^{v}	0.86	2.8900	3.507 (5)	131.00
N4—H4A···Br4^{vi}	0.89	2.82 (3)	3.604 (5)	149 (3)
N4—H4B···N1^{vii}	0.89	1.94 (4)	2.825 (8)	175 (5)
N4—H4C···Br2^{vi}	0.89	2.57 (4)	3.379 (5)	151 (4)
C23—H23···Br4^{vi}	0.93	2.9100	3.763 (7)	153.00
C10—H10···Cg(3)^{ii}	0.93	3.0070	3.631(6)	125.89
C5—H5···Cg(2)^{vi}	0.93	3.0226	3.793(7)	141.25
C21—H21···Cg(2)^{viii}	0.93	3.0833	3.758(7)	130.84
C22—H22···Cg(1)^{vii}	0.93	3.2293	3.913(7)	132.07
C2—H2···Cg(3)^{ix}	0.93	3.0402	3.791(7)	138.88
C4—H4···Cg(4)^{vi}	0.93	3.1445	3.740(7)	123.60

Symmetry codes:

(i) x−1, y, z; (ii) −x, y−1/2, −z+1/2; (iii) x−1, −y+1/2, z−1/2; (iv) −x, −y, −z; (v) x, −y+3/2, z+1/2; (vi) −x, −y+1, −z; (vii) −x, y+1/2, −z+1/2; (viii) x, y+1,z; (ix) x, y−1, z.

Cg(i): centroid of ring defined by the following atoms. i = 1: C1, C2, C3, C4, C5, C6. i = 2:, C7, C8, C9, C10, C11, C12. i = 3: C13, C14, C15, C16, C17, C18. i = 4: C19, C20, C21, C22, C23, C24.

Hirshfeld surfaces analysis

Intermolecular interactions and 3D crystal packing were studied by Hirshfeld surface analysis. The molecular Hirshfeld surface sunders space in a molecular crystal into clusters where the sum of spherical atoms for the promolecule has an electron distribution contribution that dominates the corresponding sum all over the procrystal [1]. On this surface, we can realize different properties such as d_{norm}, the electrostatic potential "ESP", the Shape Index and curvedness. d_{norm} is a standardized contact distance (eq.S1), where d_e is the distance between a point located on the surface and the nearest nucleus that is outside the surface and di is the distance from a point that is on the surface and the nearest nucleus within the surface.

$$d_{norm} = \frac{d_i - r_i^{vdw}}{r_i^{vdw}} + \frac{d_e - r_e^{vdw}}{r_e^{vdw}} \qquad (Eq.S1)$$

The red concave spots, the white and the blue areas visualized on the molecular surface mapped with d_{norm} highlight short contacts with distances, are shorter, around and longer than Van der Waals separation, respectively. The molecular Hirshfeld surface study is related to the breakdown of all intermolecular contacts described as a 2D fingerprint plot. This provides a convenient means of quantifying intermolecular interactions inside the molecular crystal [2,3].

The Hirshfeld surfaces of CdODA are illustrated in **Figure S4** showing surfaces of each molecule of the asymmetric unit that have been mapped over d_{norm} range -0.2Å to 0.9 Å. The spots visible on Hirshfeld surfaces with d_{norm} present H…Br and H…N hydrogen bond types that are observed in table S2. To quantify individual contributions of intermolecular interactions involved within the structure, the 2D fingerprint plots were decomposed. The analysis of the 2D fingerprint plots of $[H(ODA)]^+$ molecules (**Figures S5** and **S6**) reveal that the close contacts in the organic part are dominated by H…H interactions where the proportion is 37.3% for the surface of $[H(ODA)]^+$ (1) and 46.2% for the surface of $[H(ODA)]^+$(2). The percentages of contributions corresponding to C…H close contacts in the Hirshfeld surfaces are 15.2% for $[H(ODA)]^+$(1) and 12.4% for $[H(ODA)]^+$(2). This interaction appears on the surface with d_{norm} as white regions.

2.2% of Hirshfeld surface of $[H(ODA)]^+$(1) and 2.3% of $[H(ODA)]^+$(2) involve H…N/N…H close contacts. The spot (c) in **Figure S6** results from the shortest hydrogen bond N4–H4B…N1. O…H / H…O interactions contribute to the total Hirshfeld surface with 5.1% for $[H(ODA)]^+$(1) and 7.6% for $H(ODA)]^+$(2). O…C interactions contribute by 1.4% for $[H(ODA)]^+$(1), in contrast to $[H(ODA)]^+$(2) where only C…O short contacts are observed with 1.4% of the total of the surface.

The proportion of H…Br interaction between organic and inorganic parts comprises 22.1% and 17.5% of the total Hirshfeld surfaces of $[H(ODA)]^+$(1) and $[H(ODA)]^+$(2), respectively.

The breakdown of the plot of $CdBr_4$ (**figure S9**) reveals that 89.4% of surface contacts are Br…H interactions and the remaining 5.3% involves Br…C contacts. Three other close contacts are identified: Br…Br (1.4%), Br…N (0.9%) and Cd…H(2.3%). This analysis confirms that the cohesion between organic and inorganic parts is dominated by H…Br hydrogen bond interactions.

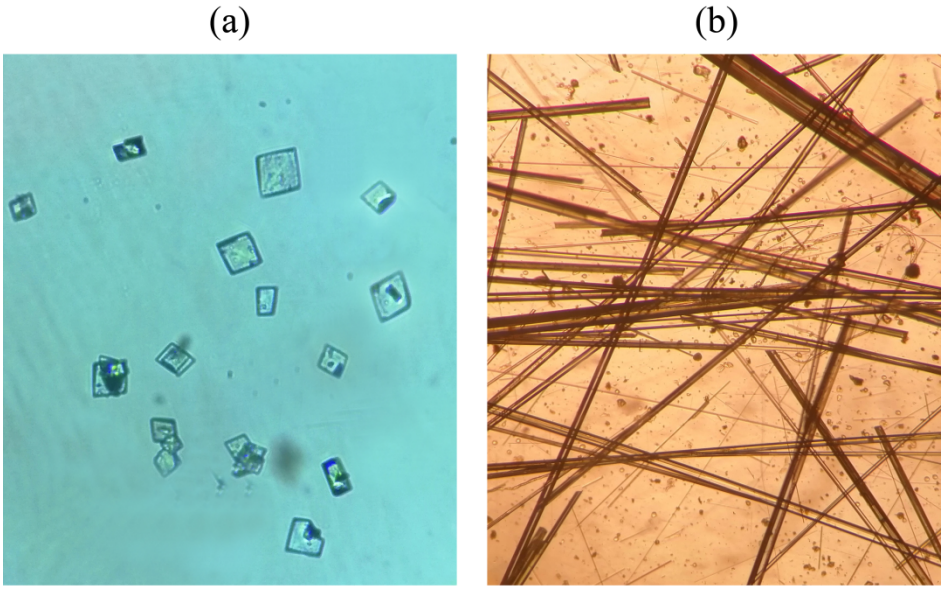

Figure S1. Digital microscopy images of CdACP (a) and CdODA (b) micro-crystals (×25)

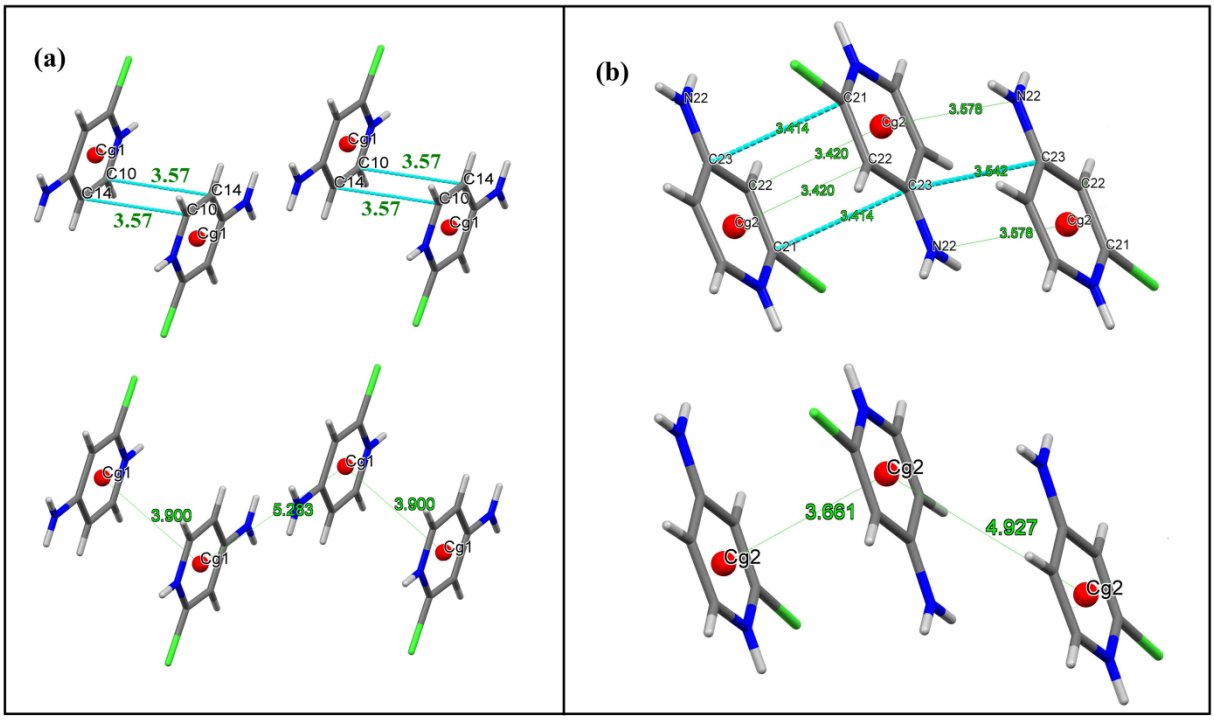

Figure S2. (a): Detailed π…π interactions with Cg1…Cg1 distances between [H(ACP)] (2) molecules and (b): Detailed π…π interactions with Cg2…Cg2 distances between [H(ACP)] (2) molecules.

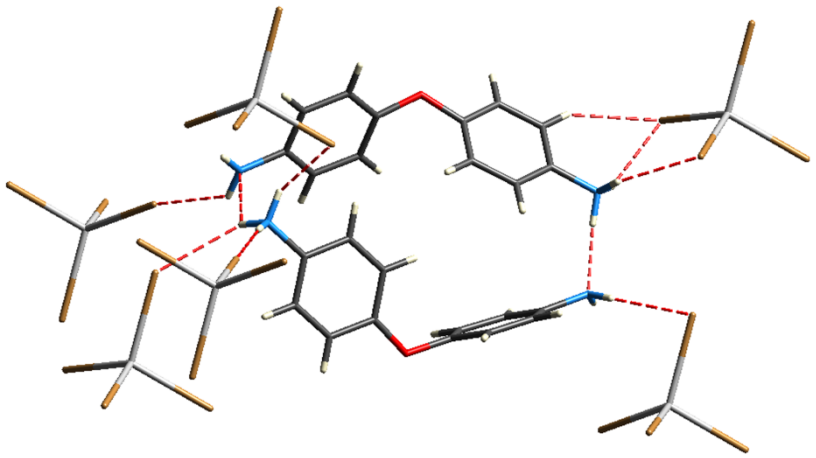

Figure S3. Hydrogen bond contacts within CdODA

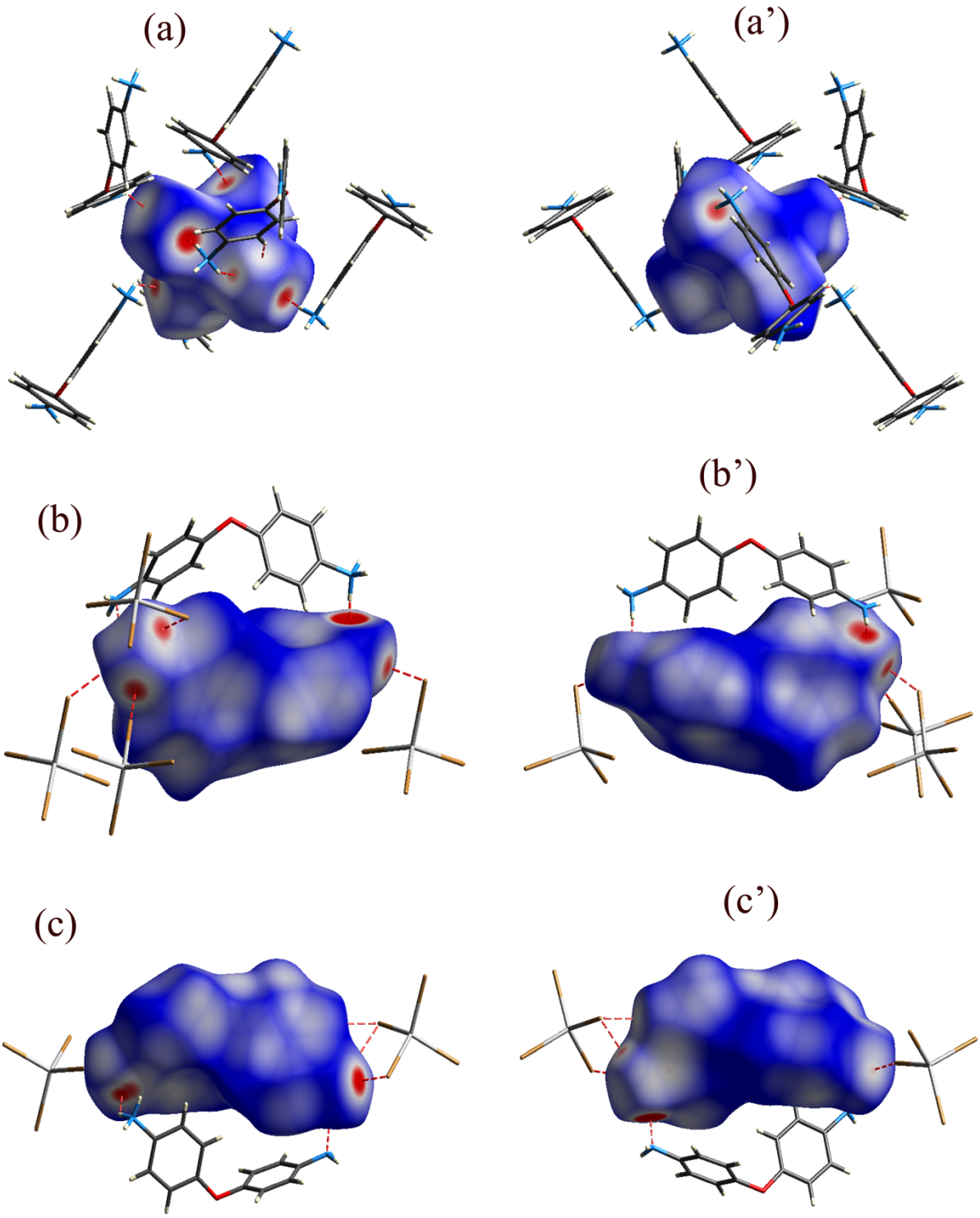

Figure S4. Front and back views of the Hirshfeld surface for molecules of the asymmetric unit of CdODA (a, a': $CdBr_4$, b, b': [H(ODA)] (1) and c, c': [H(ODA)] (2))

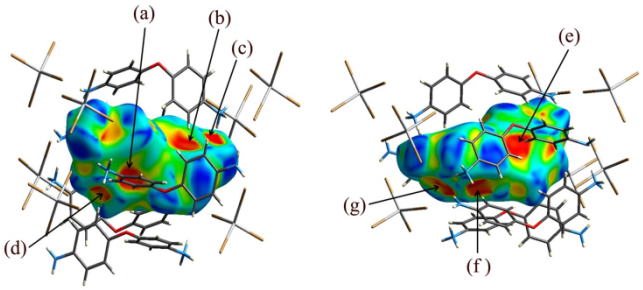

Figure S5. Hirshfeld surface of H(ODA) (1) mapped with Shape Index (-0.7 to1).

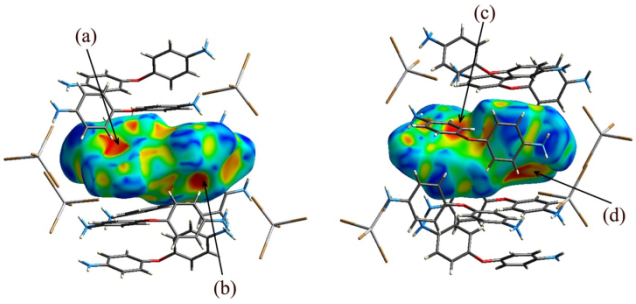

Figure S6. Hirshfeld surface of H(ODA) (2) mapped with Shape Index (-0.7 to 1).

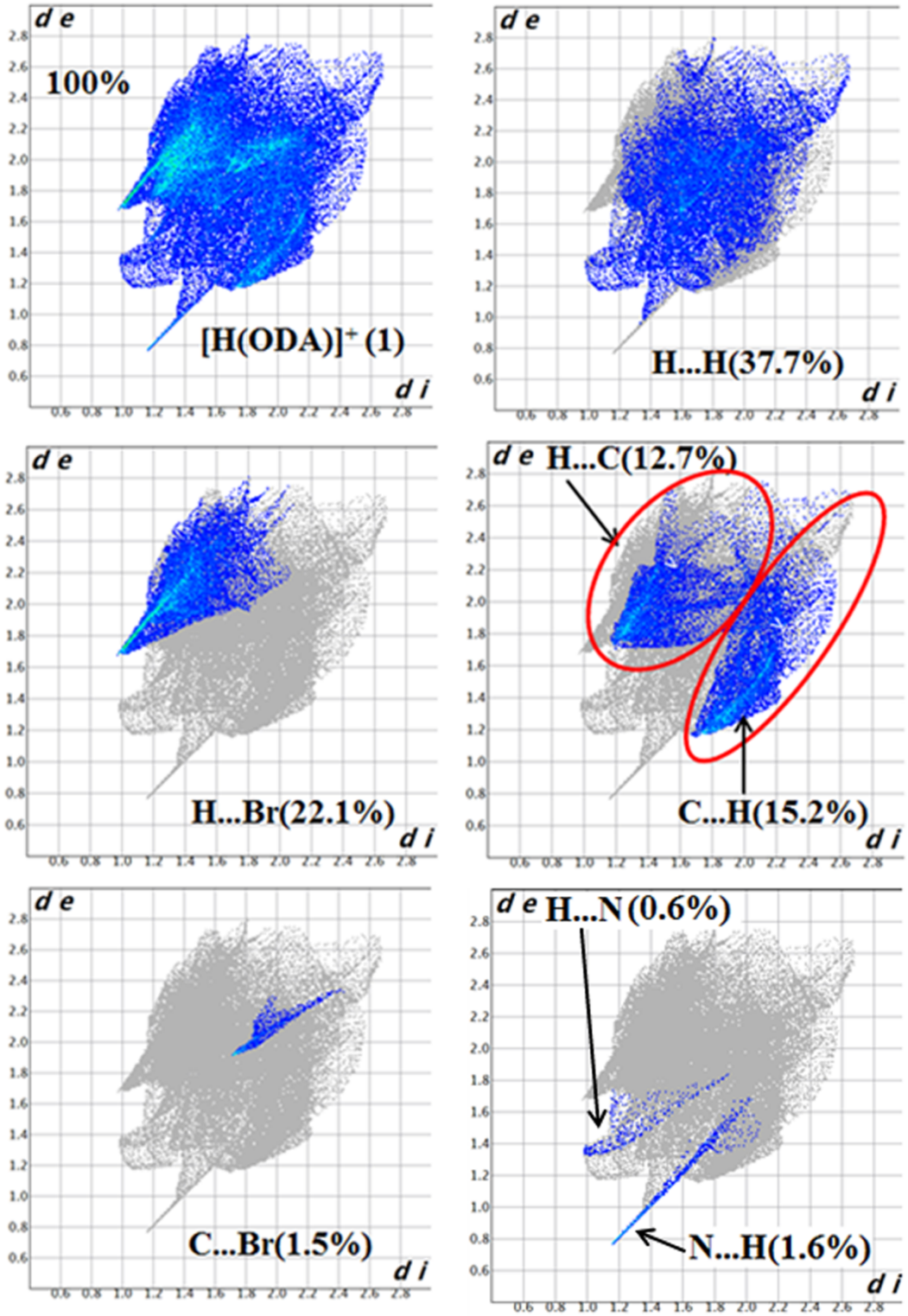

Figure S7. 2D fingerprint plots of [H(ODA)]+ (1).

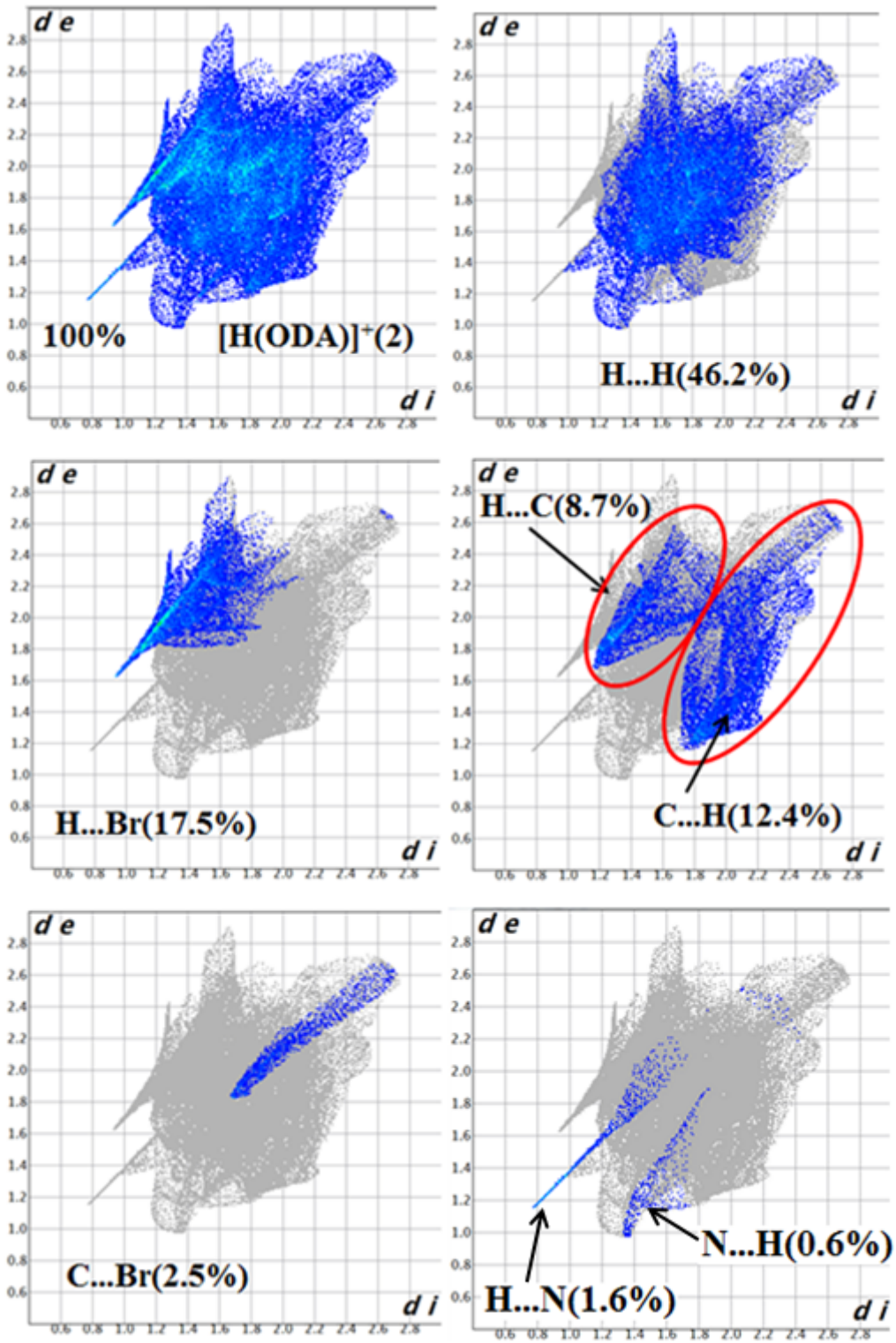

Figure S8. 2D fingerprint plots of $[H(ODA)]^+$ (2)

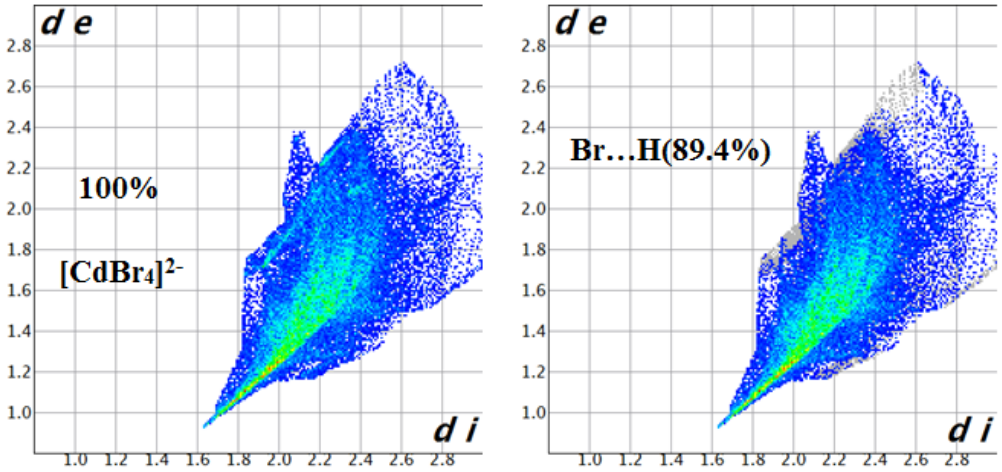

Figure S9. Fingerprint plot of $CdBr_4$ for compound (1).

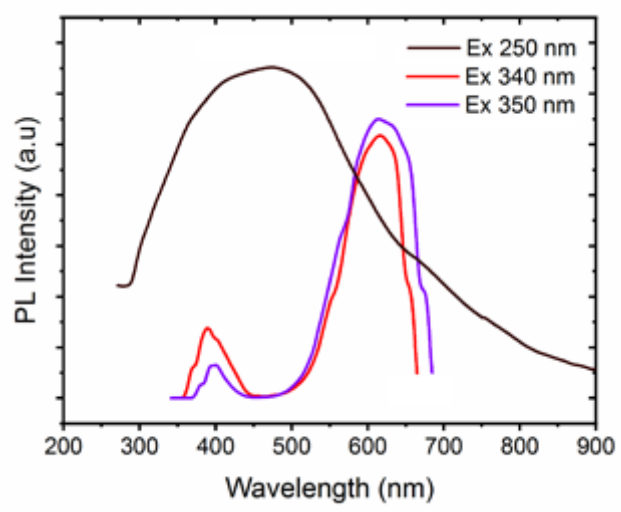

Figure S10. PL spectra of $[H(ACP)]^{+} \cdot Br^{-}$ under different excitation wavelengths.

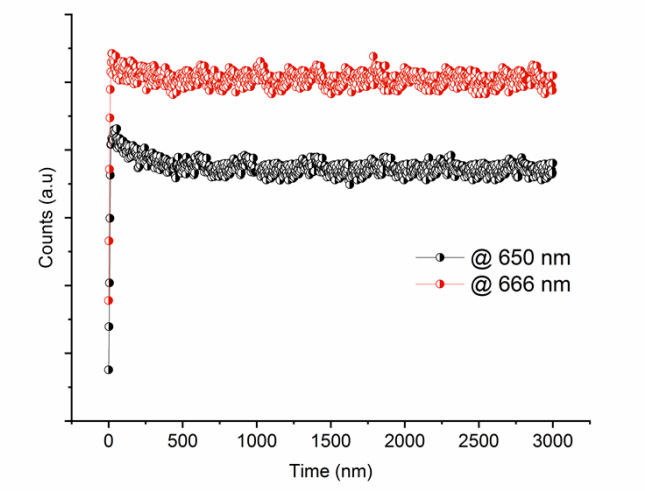

Figure S11. PL decays for CdACP collected at 650 and 666 nm under excitation wavelength λ_{exc} = 375 nm.

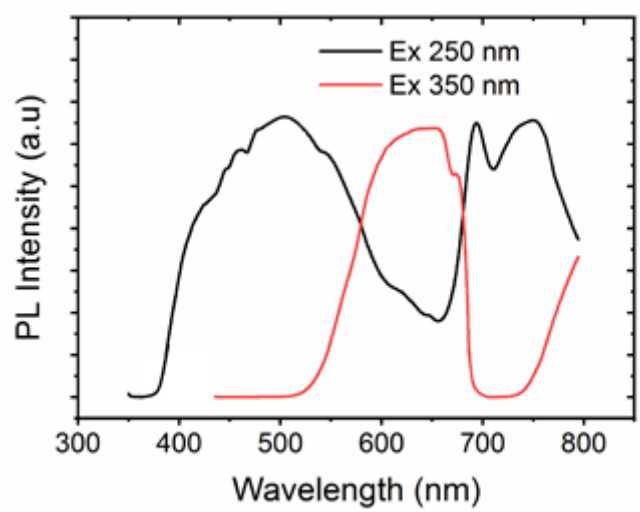

Figure S12. PL spectra of ODA amine, excited under 250 and 350 nm.

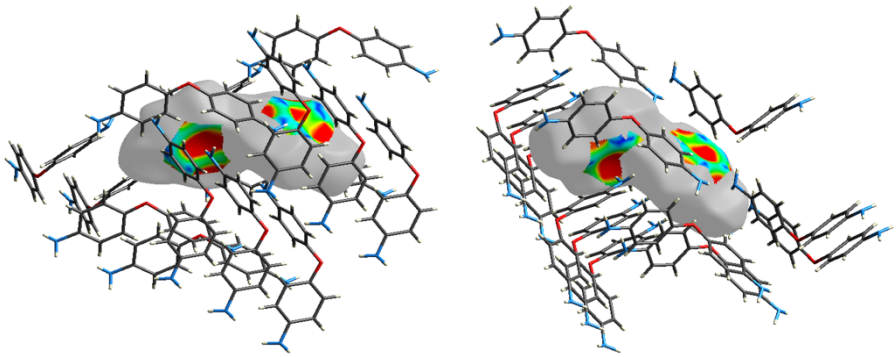

Figure S13. Visualization of C…H contacts on the Hirshfeld surface of ODA.

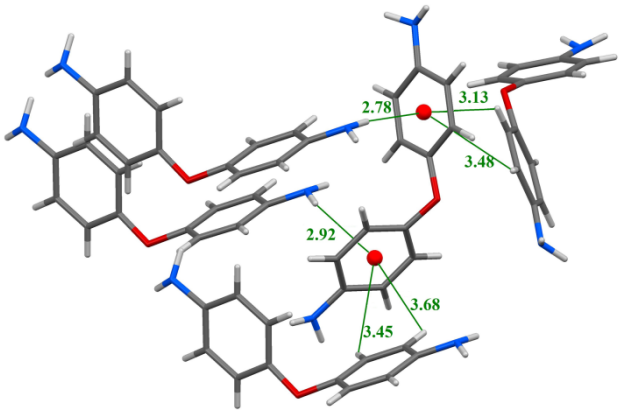

Figure S14. N-H…π and C-H…π interactions within ODA.

References

1 M. A. Spackman, *Phys. Scr.*, , DOI:10.1088/0031-8949/87/04/048103.

2 M. A. Spackman and J. J. McKinnon, *CrystEngComm*, 2002, **4**, 378–392.

3 A. Parkin, G. Barr, W. Dong, C. J. Gilmore, D. Jayatilaka, J. J. McKinnon, M. A. Spackman and C. C. Wilson, *CrystEngComm*, 2007, **9**, 648.